

Electronic Properties and Stability of [001] GaAs/InAs, GaP/InP, Ga_{1-x}In_xAs/GaAs(InAs) and Ga_{1-x}In_xP/GaP(InP)

R. H. Miwa, R. Claudino da Silva and A. C. Ferraz

Instituto de Física, Universidade de São Paulo

C.P. 20816. 01498-970, São Paulo, SP, Brasil

Received July 12, 1993

We report self-consistent electronic structure, total energy and force calculations based on the density-functional theory to study the stability of (GaAs)₃ (InAs)₃ and (GaP)₃ (InP)₃ [001] superlattices. We predict that they are unstable with respect to disproportion into zinc-blend constituents because the insufficient Ga-In and Ga-P charge transfer. Also we studied the virtual-crystal-approximation band structure concern to the Ga_{1-x}In_xAs / GaAs(InAs) and Ga_{1-x}In_xP/GaP(InP) [001] alloys superlattices and we verified the relationship of the energy bands with lattice constants and concentration on the growth process.

I. Introduction

A considerable effort has been devoted to the search for a study of heterostructures and superlattices to understand the mechanisms of strain relaxation in heteroepitaxial semiconductor layers. Strained-layer superlattices (SL's) have the additional attraction on account of the influence that built-in strains have on the resulting electronic structure. The practical disadvantage of strained-layer systems is that they are, in general, rather difficult to grow satisfactorily and there is less information than the systems made of compounds with good lattice matching^[1,2]. In the case of long-period strained-layer SL's, Osbourn^[3] has demonstrated how much systems allow independent variability of structural properties but in ultrathin SL's the interface region is a significant fraction of the total volume, and thus cause strong mixings between different zinc-blend valleys that are folded on top of each other in the SL Brillouin zone. Such effects are largely peculiar to very-short-period SL's, and thus add flexibility to these structures for band-gap engineering.

The stability of the SL's will depend on the relative energetics of the positive-definite strain contribution to the energy and the possible negative contributions due to enhanced chemical binding effects at

the interface^[4,5]. Changing the substrate lattice constant on which the SL is grown has a significant effect on the energetics of the interface matching. Also with the growth of high quality strained Ga_{1-x}In_xAs / GaAs^[6,7] and Ga_{1-x}In_xP / GaP(InP)^[8,9] [001] SL's in atmospheric and low pressure metalorganic vapour phase epitaxy (MOVPE), it has been possible to observe the effects of strain on the growth of lattice mismatched superlattices.

In this paper, we present *ab-initio* calculations to study the stability and ordering-related phenomena of the (GaAs)₃ (InAs)₃ and (GaP)₃ (InP)₃ [001] oriented SL's. As these systems and the respectively alloys can be grown by using epitaxial techniques, we also determined the electronic band structure of the SL's (Ga_{1-x}In_xAs)₃ (GaAs)₃/(InAs)₃, (Ga_{1-x}In_xP)₃ (GaP)₃/(InP)₃ and (Ga_{1-x}In_xP)₃(Ga_{y-1}In_yP)₃ along [001] direction, changing the substrate lattice constant on which the SL is grown.

II. Formation enthalpy of the [001] oriented superlattices

In order to determine the stability of the (GaAs)₃(InAs)₃ and (GaP)₃(InP)₃ SL's, we use

the density-functional theory^[10,11] with the local-density approximation for the exchange-correlation functional^[12,13]. The electron-ion interaction is described by norm-conserving, fully separable *ab-initio* pseudopotentials based on relativistic all electron calculations^[14–16]. The calculations were performed on the superlattices consisting of slabs of the semiconductors GaAs, InAs or GaP and InP, based on the [001] direction of the supercell with the lattice constants taken as the average of the theoretical bulk's lattice constants. The wave functions were expanded in plane waves with kinetic energies up to 18 Ry and the k-space integration was replaced by a sum of four special k points of the irreducible part of the Brillouin zone^[17]. To minimize errors associated with k-point sampling and plane-wave expansions, the bulk calculations were made in the superlattice geometry. The calculated equilibrium lattice constants of pure zinc-blende compounds are the following: 5.56Å for GaAs, 5.86Å for InAs, 5.36Å for GaP and 5.66Å for InP. These values reduce the mismatch between the materials on the SL to about 5.5% despite the experimental 7%.

The equilibrium atomic positions for the atoms in the superlattice's supercell were determined performing total energy and forces calculations, using an "optimized steepest descent" method for the atomic displacements together with a Car-Parrinello^[18] approach for bringing the wave functions to self-consistency. The equilibrium geometry is identified when all forces are smaller than 0.005 eV/Å, and on that positions the variations on the bond-lengths do not exceed 1%, approaching the bonds to their bulk values.

To understand the instability in size-mismatched systems, such as GaAs/InAs and GaP/InP, we follow Srivastava, Martins and Zunger^[19] and consider the formation of the SL as a three-step process. In the first step, the two constituents crystals AC and BC are compressed (dilated) when the materials change from their natural lattice constant (a_{AC} , a_{BC}) to a common equilibrium lattice constant of the superlattice (a_{\cdot}). The energy associated to that process is:

$$\begin{aligned} \Delta E_d &= \frac{1}{2} \{E[AC, a_{\cdot}] - E[AC, a_{AC}]\} \\ &+ \frac{1}{2} \{E[BC, a_{\cdot}] - E[BC, a_{BC}]\} \end{aligned}$$

In the second step the SI, formation occurs, but all the bond-lengths (R_{AC} and R_{BC}) are identical. We can imagine that step as a change of an A element by a B element on the AC structure, and a vice-versa change on the BC structure, with a charge redistribution on the SI. The energy on that process is:

$$\begin{aligned} \Delta E_c &= E[(AC)(BC), a_{eq}, R_{AC} = R_{BC}] \\ &- \frac{1}{2} \{E[(AC), a_{eq}, R_{AC}] + E[(BC), a_{eq}, R_{BC}]\} \end{aligned}$$

Finally the third step consists of the internal structural distortions. The bond-lengths between the AC elements (R_{AC}) and the BC elements (R_{BC}) have now new values, R_{AC}^{eq} and R_{BC}^{eq} . The energy associated to that relaxation process is:

$$\begin{aligned} \Delta E_r &= E[(AC)(BC), a_{eq}, R_{AC}^{eq}, R_{BC}^{eq}] \\ &- E[(AC)(BC), a_{eq}, R_{AC} \equiv R_{BC}] \end{aligned}$$

The formation enthalpy ΔH , will be the sum of the energies involved on the three steps:

$$\begin{aligned} \Delta H &= E[(AC)(BC), a_{eq}, R_{AC}^{eq}, R_{BC}^{eq}] \\ &- \frac{1}{2} \{E[(AC), a_{AC}] + E[(BC), a_{BC}]\} \end{aligned}$$

For lattice-mismatched systems, the largest contribution for ΔH comes from ΔE_d which is always positive and from ΔE_r which is negative. ΔE_d corresponds to the work necessary to bring A-C and B-C bond lengths from their equilibrium values to the common value, so ΔE_d becomes bigger as the mismatch increases and only part of this energy is recovered by ΔE_r ^[20]. In lattice-matched systems, such as AlAs/GaAs, the strain energy ΔE_d vanishes and the entire formation enthalpy is given by the chemical energy associated with ΔE_r and ΔE_c . The use of the averaged lattice constant between GaAs/InAs and GaP/InP is justified by the fact that the SL lattice constant follow the Vegard's law within 0.2%. Considering that our theoretical lattice constants are smaller than the experimental ones

Table I. Formation enthalpy ΔH and its decomposition ΔE_d , ΔE_c and ΔE_r for [001] 3×3 superlattices. All the values are in meV/atom.

	ΔE_d	ΔE_c	ΔE_r	ΔH
(GaAs) ₃ (InAs) ₃	33.4	2.1	-21.3	14.2
(GaP) ₃ (InP) ₃	41.4	1.9	-28.0	15.3

and the mismatches between both superlattices are reduced to around 5.5% (experimental value is 7%), we are underestimating the contribution of the deformation energy ΔE_d .

The calculated values of the formation enthalpy and its individual contributions ΔE_d , ΔE_c and ΔE_r are reported in Table I for the (GaAs)₃(InAs)₃ and (GaP)₃(InP)₃ SL's. Both SL's are unstable towards disproportionation into zinc-blend constituents. Dandrea et al.^[21] and Boguslawski^[20] calculated self-consistently in the the local-density approximation and nonlocal pseudopotential plane-wave method the superlattices (GaAs)₁(InAs)₁, grown in the [001] orientation and found the values of 22.8 and 20.9 meV/atom respectively for ΔH . The results obtained by Srivastava^[22] and reference 20, also using self-consistent pseudo potentials and [001] orientation, for (GaP)₁(InP)₁ were 22.8 and 28.9 meV/atom respectively. Dandrea still concluded that long-period [001] SL has lower energy formation but higher energy than the disordered alloy (12.8 meV/atom for Ga_{0.5}In_{0.5}As and 16.7 meV/atom for Ga_{0.5}In_{0.5}P) and unstable with respect to phase separation ($\Delta H > 0$).

Our calculated ΔH values for the SL's (GaAs)₃(InAs)₃ and (GaP)₃(InP)₃ have shown that the excess energy remains positive for isovalent SL's in the [001] orientation, suggesting their thermodynamic instability. The point now is that the values are of the same order of the mixing enthalpy of the disordered alloy. On the other hand, the direction of charge transfer between two different atoms is predicted from their difference in electronegativity; that is, charge is transferred from a less electronegative atom to a more electronegative one. Some results^[19] for (GaP)₁(InP)₁ confirm the prediction of the electronegativity rule show-

ing that the charge is transferred from the InP layers to the GaP ones. However, Ohno^[23] obtained an opposite direction of charge transfer between In and Ga atoms for the (GaAs)₁(InAs)₁ SL's: the charge transfer from GaAs layers to InAs layers. In view of the above results, the electronegativity rule that contribute for the chemical energy on the formation enthalpy, cannot alone play the role in determining the stability of superlattice structures.

From the previous results, we can see that the large contribution to ΔH is from the strain, so the less unstable SL's should be grown on an alloy substrate in order to reduce strain effect. Thus, ordered alloy superlattices can exhibit stability, with respect to disproportionation and disordering, since ordered phases accommodate the associated strain better than do disordered phases.

III. Electronic band structure of the ordered [001] SL's alloys

Considering that global understanding of the phase relationships and stability, we have performed calculations of (Ga_{1-x}In_xAs)₃(GaAs)₃, (Ga_{1-x}In_xAs)₃(InAs)₃, (Ga_{x-1}In_xP)₃(GaP)₃, (Ga_{1-x}In_xP)₃(InP)₃ and (Ga_{0.6}In_{0.4}P)₃(Ga_{0.4}In_{0.6}P)₃ SL's oriented on the [001] direction, to determine the trends of band-structure.

While the norm-conserving pseudopotential is formed from the atomic wave functions of all electrons in an atom and suitable to the determination of the ground state properties, the empirical pseudopotential, which is determined so as to reproduce atomic and solid properties, is suited to analyzing excited state properties of an atom or a solid. So we used the former to determine the stability of ground state properties and for a simple but reliable approach to both valence and conduction band, we used the local pseudopotential method to calculate the electronic band structures and optical properties of the semiconductor superlattices. The semiempirical ionic pseudopotentials for Ga, In, As and P were taken from Taguchi^[24] and Ferraz^[25] within the $X\alpha$ scheme. All wave vectors up to a kinetic energy of 4.41 Ry were considered exactly for all

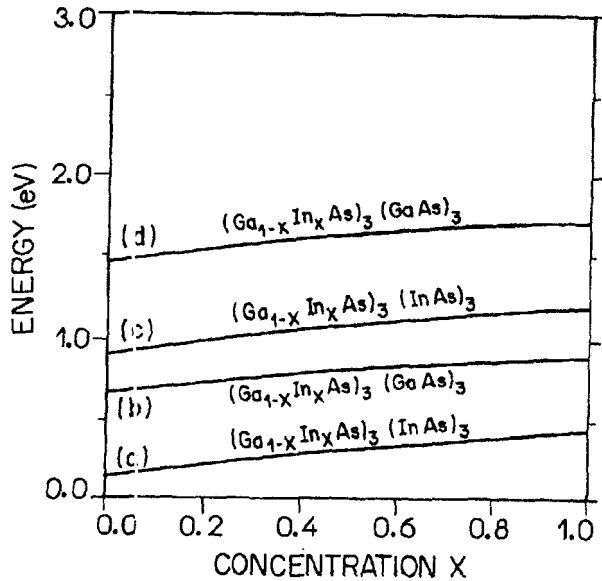


Figure 1: Energy gap versus alloy concentration for the superlattices $(\text{Ga}_{1-x}\text{In}_x\text{As})_3(\text{GaAs})_3$ and $(\text{Ga}_{1-x}\text{In}_x\text{As})_3(\text{InAs})_3$ along [001] direction. The labels a, b, c and d refer to growth on different lattice constants as follow: a) a^{InAs} , b) and c) $a = \frac{1}{2}(a^{\text{InAs}} + a^{\text{GaAs}})$, d) a^{GaAs} .

the structure and as the previous calculations, a set of special points was used for sampling the k-space. The virtual-crystal approximation (VCA) was used for the alloys $A_{1-x}B_xC$, replacing the microscopically inhomogeneous distribution of A and B atoms with a lattice of identical fictitious atoms whose properties represent a composition with appropriate weighted average of the A and B pseudopotentials. The experimental lattice constants were taken for GaAs (5.653Å), InAs (6.058Å), GaP (5.451Å) and InP (5.869Å), and for the alloys we considered the Vegard's law. The obtained energy gaps were found as 1.46 eV (GaAs), 0.44 eV (InAs), 2.29 eV (GaP) and 1.32 eV (InP) and for the alloys the values also agree very well with experimental results.

All SL structures were relaxed up to the equilibrium atomic positions in the unit cell, that minimize the total energy. As in the case of the *ab-initio* calculations of part II, the variations of the bond-lengths were around 1% to the relaxed SL, with the displacements approaching the III-V bonds to their bulk values.

Figures 1 and 2 show the calculated energy gap related to the SL's 3×3 along [001] direction, for the ternary alloys $\text{Ga}_{1-x}\text{In}_x\text{As}$ and $\text{Ga}_{1-x}\text{In}_x\text{P}$, and the respective III-V compounds GaAs/InAs and GaP/InP.

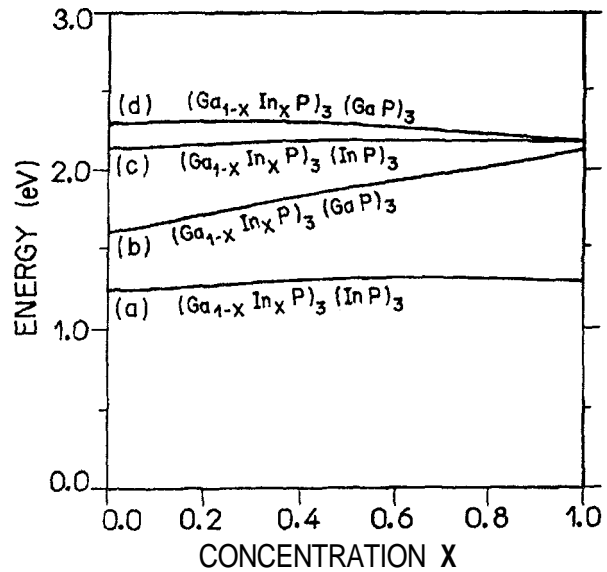


Figure 2: Energy gap versus alloy concentration for the superlattices $(\text{Ga}_{1-x}\text{In}_x\text{P})_3(\text{GaP})_3$ and $(\text{Ga}_{1-x}\text{In}_x\text{P})_3(\text{InP})_3$ along [001] direction. The labels a, b, c and d refer to growth on different lattice constants as follow: a) a^{InP} , b) and c) $a = \frac{1}{2}(a^{\text{InP}} + a^{\text{GaP}})$, d) a^{GaP} .

All the curves present an almost linear behavior. The largest gap is related to the compound that has the smallest lattice constant (GaAs, GaP), while the smallest gap is related to that of largest lattice constant (InAs, InP). The SL's grown on that compounds follow the same trend. $(\text{Ga}_{1-x}\text{In}_x\text{As})_3(\text{InAs})_3$ and $(\text{Ga}_{1-x}\text{In}_x\text{P})_3(\text{InP})_3$ grown on InAs and InP respectively, have the smallest gaps for all the alloy concentration, while the SL's $(\text{Ga}_{1-x}\text{In}_x\text{As})_3(\text{GaAs})_3$ and $(\text{Ga}_{1-x}\text{In}_x\text{P})_3(\text{GaP})_3$ have the largest gaps when grown on GaAs and GaP. The SL's grown on the average lattice constants present intermediate gaps but, now there is an inversion on the trend: $(\text{Ga}_{1-x}\text{In}_x\text{As})_3(\text{GaAs})_3$ and $(\text{Ga}_{1-x}\text{In}_x\text{P})_3(\text{GaP})_3$ have an energy gap lower than $(\text{Ga}_{1-x}\text{In}_x\text{As})_3(\text{InAs})_3$ and $(\text{Ga}_{1-x}\text{In}_x\text{P})_3(\text{InP})_3$ respectively, when grown on the average lattice constants. All SL's exhibit direct transition to the lowest conduction state except $(\text{Ga}_{1-x}\text{In}_x\text{P})_3(\text{GaP})_3$ grown on GaP lattice constant, that present an indirect transition. Another characteristic of these SL's is that there is a slowly decreasing of energy gap as In concentration increases, while for all other SL's the gap increases with In concentration on the alloys.

Considering the most favorable structures of SL's

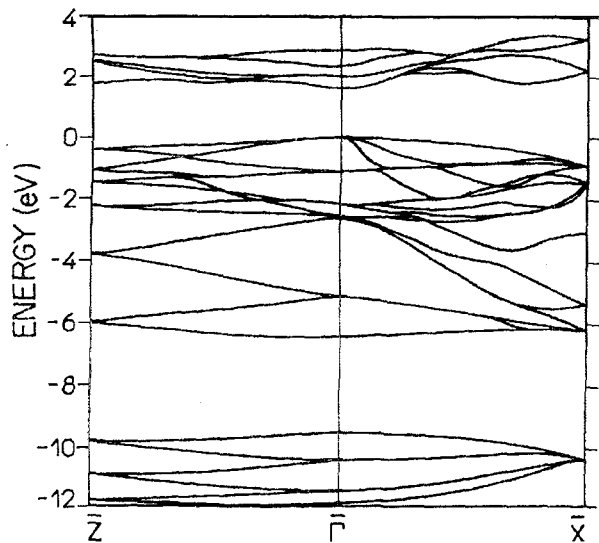


Figure 3: Energy-band structure of the $(\text{Ga}_{0.8}\text{In}_{0.2}\text{As})_3(\text{GaAs})_3$ superlattice along $[001]$ direction based on GaAs.

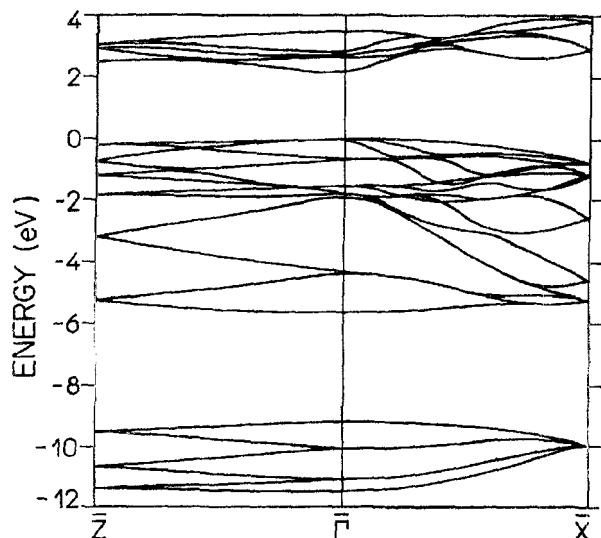


Figure 4: Energy-band structure of the $(\text{Ga}_{0.6}\text{In}_{0.4}\text{P})_3(\text{Ga}_{0.4}\text{In}_{0.6}\text{P})_3$ superlattice along $[001]$ direction based on a substrate with lattice constant averaged between the two alloys.

with respect to stability, as mentioned at part II, we calculated the dispersion of electronic states along the superlattice growth direction $[001]$ for $(\text{Ga}_{0.8}\text{In}_{0.2}\text{As})_3(\text{GaAs})_3$ on the GaAs lattice constant and for $(\text{Ga}_{0.6}\text{In}_{1.0}\text{P})_3(\text{Ga}_{0.4}\text{In}_{0.6}\text{P})_3$ on the average lattice constant between the two alloys. Figures 3 and 4 show the energy-band structure of these 3×3 full relaxed SL's along the high-symmetry axes. X correspond to X point in the fcc Brillouin zone and \bar{Z} is related to the growth direction. In Fig. 3 the energy-gap is 1.52 eV and in Fig. 4 is 2.19 eV. In both case the value of the energy gap is just the average gap between the compounds that compose the SL at that lattice constant. The dispersions are identical for the two SL's even on details in the valence and conduction states. The unique difference is the energy-gap.

In summary, we have shown that the lattice-mismatched $(\text{GaAs})_3(\text{InAs})_3$ and $(\text{GaP})_3(\text{InP})_3$ SL's are unstable against phase segregation. The formation enthalpy of these systems is dominated by the strain contribution ΔE_d . In order to reduce strain effects the alloy SL's should be less unstable. The substrate lattice constant on which the SL is grown strongly affects the electronic band-structure. For all SL's the gap increases with In concentration on the alloys, except for the SL $(\text{Ga}_{1-x}\text{In}_x\text{P})_3(\text{GaP})_3$ grown on GaP lattice constant.

References

1. J. Arriaga, G. Armelles, M. C. Muñoz, J.M. Rodrigues, P. Castrillo, M. Recio, V. R. Velasco, F. Briones and F. Garcia - Moliner, Phys. Rev. B 43, 2050 (1991).
2. J. Arriaga, M. C. Muñoz, V. R. Velasco and F. Garcia - Moliner, Phys. Rev. B 43, 9626 (1991).
3. G. C. Osbourn, J. Vac. Sci. Technol. B 1, 379 (1953).
4. J. S. Nelson and I. P. Batra, Phys. Rev. B 39, 3250 (1989).
5. D. B. Laks and A. Zunger, Phys. Rev. B 45, 14177 (1992).
6. K. J. Monserrat, J. N. Tothill, J. Haigh and R. H. Moss, J. Cryst. Growth 93, 466 (1988).

- 7 K. L. Cavanagh, M. A. Capasso, L. W. Hobbs, J. C. Barbour, P. M. J. Marée, W. Schaff, J. W. Mayer, D. Petit, J. M. Woodal, J. A. Stroschio and R. M. Feenstra, *J. Appl. Phys.* **64**, 4843 (1988).
- 8 W. Korber and K. W. Benz, *J. Cryst. Growth* **73**, 179 (1985).
- 9 A. Beisaada, A. Chennouf, R. W. Cochrane, R. Leonel i, P. Cova and R. A. Masut, *J. Appl. Phys.* **71**, 1737 (1992).
- 10 P. Hohenberg and W. Kohn, *Phys. Rev.* **136**, B864 (1964).
- 11 W. Kohn and L. J. Sham, *Phys. Rev.* **140**, A1133 (1965).
- 12 D. M. Ceperley and B. I. Alder, *Phys. Rev. Lett.* **45**, 566 (1980).
- 13 P. Perdeu and A. Zunger, *Phys. Rev. Lett.* **B 23**, 5048 (1981).
- 14 G. B. Bachlet, D. R. Hamann and M. Schluter, *Phys. Rev. B* **26**, 4199 (1982).
- 15 L. Kleinman and D. M. Bylander, *Phys. Rev. Lett.* **43**, 1425 (1982).
- 16 S. Gonze, R. Stuinpf and M. Scheffler, *Phys. Rev. B* **44**, 5503 (1991).
- 17 H. J. Monkhorst and J. D. Pack, *Phys. Rev. B* **13**, 5158 (1976).
- 18 R. Car and M. Parrinello, *Phys. Rev. Lett.* **55**, 2471 (1985).
- 19 G. P. Srivastava, J. L. Martins and A. Zunger, *Phys. Rev. Lett.* **31**, 2561 (1985); D. M. Wood, S. H. Wei and A. Zunger, *Phys. Rev. B* **37**, 1342 (1988).
- 20 P. Boguslawski and A. Baldereschi, *Phys. Rev. B* **39**, 8055 (1989).
- 21 R. G. Dandrea, J. E. Bernard, S. H. Wei and A. Zunger, *Phys. Rev. Lett.* **64**, 36 (1990).
- 22 G. P. Srivastava, J. L. Martins and A. Zunger, *Phys. Rev. B* **38**, 12694 (1988).
- 23 T. Omino, *Phys. Rev. B* **38**, 13191 (1988).
- 24 A. Taguchi and T. Ohno, *Phys. Rev. B* **36**, 1696 (1987).
- 25 A. C. Ferraz and S. K. de Figueiredo, *Superlatt. and Microstruc.* **10**, 193 (1991).